Draft version May 28, 2018
Preprint typeset using LaTeX style emulateapj v. 08/22/09

IMPROVED DISTANCES TO TYPE IA SUPERNOVAE WITH TWO SPECTROSCOPIC SUBCLASSES

X. Wang[1,2], A. V. Filippenko[1], M. Ganeshalingam[1], W. Li[1], J. M. Silverman[1], L. Wang[3], R. Chornock[1], R. J. Foley[1,4,5], E. L. Gates[6], B. Macomber[1], F. J. D. Serduke[1], T. N. Steele[1], and D. S. Wong[1]

Draft version May 28, 2018

ABSTRACT

We study the observables of 158 relatively normal Type Ia supernovae (SNe Ia) by dividing them into two groups in terms of the expansion velocity inferred from the absorption minimum of the Si II λ6355 line in their spectra near B-band maximum brightness. One group ("Normal") consists of normal SNe Ia populating a narrow strip in the Si II velocity distribution, with an average expansion velocity $\langle v \rangle = 10,600 \pm 400$ km s^{-1} near B maximum; the other group ("HV") consists of objects with higher velocities, $v \gtrsim 11,800$ km s^{-1}. Compared with the Normal group, the HV one shows a narrower distribution in both the peak luminosity and the luminosity decline rate Δm_{15}. In particular, their $B-V$ colors at maximum brightness are found to be on average redder by $\sim$0.1 mag, suggesting that they either are associated with dusty environments or have intrinsically red $B-V$ colors. The HV SNe Ia are also found to prefer a lower extinction ratio $R_V \approx 1.6$ (versus $\sim$2.4 for the Normal ones). Applying such an absorption-correction dichotomy to SNe Ia of these two groups remarkably reduces the dispersion in their peak luminosity from 0.178 mag to only 0.125 mag.

Subject headings: cosmology: observations – distance scale – dust, extinction – supernovae: general

1. INTRODUCTION

Type Ia supernovae (SNe Ia) play important roles in observational cosmology, with the most compelling evidence for cosmic acceleration coming from their distance measurements (Riess et al. 1998; Perlmutter et al. 1999). Most SNe Ia are found to show similar spectral and photometric behavior (e.g., Suntzeff 1996; Filippenko 1997), suggesting a relatively homogeneous origin — probably an accreting carbon-oxygen white dwarf in a binary system (e.g., Hillebrandt & Niemeyer 2000). Yet the presence of some extreme events such as SN 1991T (Filippenko et al. 1992a) and SN 1991bg (Filippenko et al. 1992b), and the truly peculiar SN 2002cx-like objects (Li et al. 2003), may indicate multiple channels producing the thermonuclear explosion of SNe Ia.

Diversity is observed even among the relatively normal SNe Ia. At a given phase there is a large spread among the absorption blueshifts of their spectral features (e.g., Benetti et al. 2005, hereafter B05), and there are also differences in line strengths. The scatter comes primarily from objects showing high photospheric velocities. Representative examples are SNe 2002bo, 2002dj, 2004dt, and 2006X (Benetti et al. 2004; Pignata et al. 2008; L. Wang et al. 2006; Wang et al. 2008a, hereafter W08a); the Si II velocities near B-band maximum light are higher than those of the normal SNe Ia by $\sim$2500–5500 km s^{-1}. Such SNe Ia are defined as a subclass in terms of the temporal velocity gradient of Si II (B05), and also grouped by Branch et al. (2006) according to the equivalent width (EW) of the Si II λ6355 and Si II λ5972 absorptions lines. The origin of the high expansion velocities is debated, with a conventional mechanism being a density/abundance enhancement in the outer ejecta (e.g., Tanaka et al. 2008). A statistical study of the observables may allow one to penetrate deeper into their explosion physics and understand their impact on the use of SNe Ia to measure the properties of dark energy.

The main thrust of this *Letter* is to show that SNe Ia with high expansion velocities may have a lower extinction ratio with respect to the normal ones. Using two different values of R_V in their brightness corrections, the utility of SNe Ia for cosmological distance determinations can be substantially increased.

2. SPECTROSCOPIC CLASSIFICATION OF SNE IA

The sample in our study includes most of the SNe Ia available in the literature and in our database[7]; it consists of 158 relatively normal SNe Ia with good photometry and generally at least one spectrum within one week after B maximum. The spectral data are primarily from Matheson et al. (2008, hereafter M08) and our own database (Silverman et al., in prep., hereafter S09). For a few objects, the spectral parameters were also taken from B05, Branch et al. (2009), and the IAU Circulars. Table 1 lists the observed parameters as well as the classifications of the SNe Ia.

2.1. *Expansion Velocity from Si IIλ6355*

Si II λ6355 is one of the strongest features in optical/near-infrared spectra of SNe Ia; the blueshift of

[1] Department of Astronomy, University of California, Berkeley, CA 94720-3411, USA.;wangxf@astro.berkeley.edu.
[2] Physics Department and Tsinghua Center for Astrophysics (THCA), Tsinghua University, Beijing, 100084, China.
[3] Physics Department, Texas A&M University, College Station, TX 77843.
[4] Harvard-Smithsonian Center for Astrophysics, 60 Garden Street, Cambridge, MA, 02138.
[5] Clay Fellow.
[6] Lick Observatory, P.O. Box 85, Mount Hamilton, CA 95140.

[7] Peculiar objects such as SN 1991T and SN 1991bg were not included in this sample. The criteria used to identify the 91T-like objects include weak Si II absorption and prominent Fe III lines in the near-maximum spectra, while identification of the 91bg-like events relies on the presence of obvious Ti II absorption or a very deep Si II λ5972 feature (the Si line-depth ratio [$\Re$(Si II); Nugent et al. 1995] is larger than 0.50). The list of the peculiar events can be provided upon request.

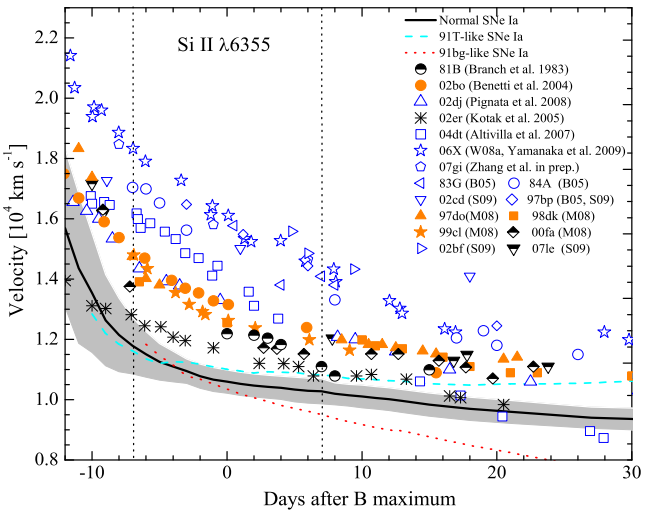

FIG. 1.— Temporal evolution of the expansion velocity inferred from the blueshift of the Si II λ6355 absorption minimum. The solid line shows the mean evolution obtained from 10 well-observed Normal SNe Ia, and the gray region represents the 1σ uncertainty; the dashed and dotted lines illustrate the evolution of the mean velocity for SN 1991T-like and SN 1991bg-like events, respectively (the data sources are M08 and S09). Overplotted is part of the HV sample, while SN 2002er may be a transitional object linking the HV and Normal groups.

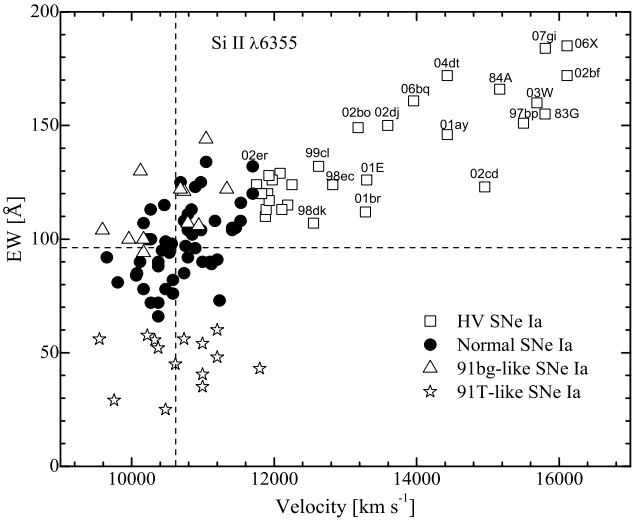

FIG. 2.— EW of Si II λ6355 absorption versus the expansion velocity, measured from spectra taken within ±3 day of B maximum, for SNe Ia of different subtypes. The vertical and horizontal lines mark the respective locations of the mean velocity and EW of the Normal SNe Ia.

its absorption minimum has often been used to diagnose the diversity among SNe Ia. B05 distinguished SNe Ia having a high Si II temporal velocity gradient (HVG) from those with a low Si II temporal velocity gradient (LVG). However, relatively few objects have the multi-epoch spectra (covering phases from maximum brightness to a few weeks thereafter) necessary for measurement of such a velocity gradient. As the HVG SNe Ia generally have faster expansion velocities than the LVG ones, we may nominally divide the SN Ia sample into "Normal" and "HV" groups according to the observed velocity of Si II λ6355.

Based on the Si II velocity distribution of 10 well-observed Normal SNe Ia[8], we derive their mean velocity from $t = -12$ day to $+30$ day. The evolution of the mean velocity is shown in Figure 1, where the gray area indicates 1σ uncertainty obtained through Monte Carlo simulations. After maximum brightness, the velocity evolves nearly in a linear fashion, with a gradient of about 40 km s^{-1} day^{-1} and a typical scatter $\sim \pm 400$ km s^{-1}. The large scatter shown before $t \approx -7$ day is caused by detached HV features at the earliest epochs. In comparison with the lower velocity and homogeneous distribution seen in the Normal SNe Ia, the expansion velocities of the HV SNe Ia are higher but more scattered, with a faster decay. The highest contrast in the Si II velocity between these two groups occurs within one week from the maximum brightness. After $t \approx +7$ day, the velocities of some HV SNe Ia are comparable to those of the Normal ones. We thus use the velocity measured within one week from the maximum to subclassify our sample; the value obtained with the spectrum closer to B maximum is adopted when multi-epoch measurements are available. By applying a 3σ selection criterion, 55 of the 158 objects were identified as HV SNe Ia. We note that there is no sharp division between these two groups when the velocity approaches a lower value (see also Fig. 2), so blending could occur to some extent.

[8] The sample includes SNe 1989B, 1994D, 1997dt, 1998aq, 1998bu, 1999ee, 2003cg, 2003du, 2004eo, and 2005cf (Barbon et al. 1990; Patat et al. 1996; M08; Branch et al. 2003; Hamuy et al. 2002; Elisa-Rosa et al. 2006; Stanishev et al. 2007; Pastorello et al. 2007; Garavini et al. 2007; Wang et al. 2009).

2.2. *Equivalent Width of Si II λ6355*

An alternative way to quantify the diversity of SNe Ia is through the line-strength ratio (e.g., Nugent et al. 1995) or the equivalent width (EW) of some features (e.g., Hachinger et al. 2006). Based on the EW of the absorption near Si IIλ5972 and Si IIλ6355, Branch et al. (2006, 2009) suggest dividing the SN Ia sample into four groups: cool (CL), shallow silicon (SS), core normal (CN), and broad line (BL); their CL and SS groups consist mainly of peculiar events such as SN 1991bg and SN 1991T, respectively. Compared with the Branch CN SNe Ia, our definition of the Normal sample is wider, while their BL objects overlap well with our HV sample.

Figure 2 shows a plot of the EW versus the velocity of Si II λ6355 absorption, obtained for SNe Ia with spectra near B maximum. One can see that the Si II absorption is generally strong in the HV subclass, typically with $EW \gtrsim 100$ Å, and the strength of the absorption correlates with the expansion velocity. In principle, strong absorption at high velocity can be caused by an enhancement of abundance or density in the outermost layers, perhaps due to an extended burning front (B05) or an interaction with circumstellar material (e.g., Gerardy et al. 2004). The continuous distribution of the EW and velocity between the HV and Normal SNe Ia suggests that such an enhancement process occurs to different degrees with considerable probability. This could be interpreted as a line-of-sight effect if the high velocities are caused by aspherical structures, such as a thick torus, as evidenced by the intrinsically large polarization detected for HV objects (e.g., L. Wang et al. 2006).

3. PHOTOMETRIC PROPERTIES OF THE HV AND NORMAL SNE IA

Given the spectroscopic diversity of the HV and the Normal groups addressed in §2, it is interesting to com-

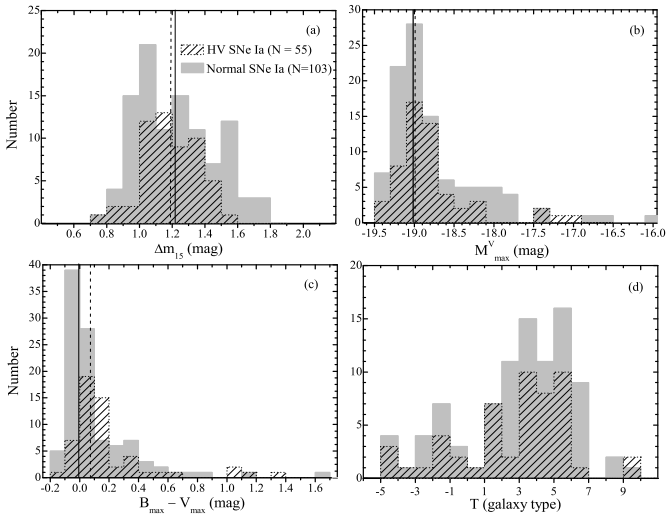

FIG. 3.— Histogram distribution of Δm_{15}, the V-band absolute magnitudes, the $B_{\rm max}-V_{\rm max}$ colors, and the T-types of the host galaxies. Two vertical lines in panels (a), (b), and (c) mark the respective mean values of the observables for the Normal (solid) and HV (dashed) SNe Ia with $B_{\rm max}-V_{\rm max}<0.20$ mag.

pare their photometric behaviors. The peak magnitude and decline rate Δm_{15} (Phillips 1993) are taken from the literature (e.g., Reindl et al. 2005; Hicken et al. 2008) or estimated from our own photometry (Ganeshalingam et al., in prep.) obtained primarily with the Lick Observatory 0.76-m Katzman Automatic Imaging Telescope (KAIT; Filippenko et al. 2001) and the 1-m Nickel reflector. Distances to the SNe are computed by using the redshifts of their host galaxies, in the reference frame of the 3 K cosmic microwave background radiation for samples at redshift $z\gtrsim0.01$ or corrected to a self-consistent Virgocentric infall of 220 km s^{-1} for closer ones, with a Hubble constant $H_0=70.5$ km s^{-1} Mpc^{-1} (Komatsu et al. 2009). A peculiar-velocity component of 300 km s^{-1} is included in the distance-modulus uncertainties. Cepheid distances are adopted whenever available (see X. Wang et al. 2006, and references therein).

3.1. *Luminosity and the Secondary Parameters*

Shown in Figure 3 are the distributions of the V-band peak absolute magnitudes $M^V_{\rm max}$, the $B_{\rm max}-V_{\rm max}$ color, Δm_{15}, and the morphological T-type of the host galaxy (de Vaucouleurs et al. 1991, hereafter RC3) for the HV and Normal SNe Ia. Both $M^V_{\rm max}$ and $B_{\rm max}-V_{\rm max}$ were K-corrected (e.g., Jha et al. 2007) and dereddened by the Galactic reddening using the full-sky maps of dust infrared emission (Schlegel et al. 1998).

As can be seen from Figure 3a, the decline rate of the HV SNe Ia exhibit a narrower distribution relative to the Normal group. Although they include events with small Δm_{15}, no HV objects were found at $\Delta m_{15}>1.6$. A similar narrow distribution is seen in their V-band absolute magnitudes (Fig. 3b), with exceptions for a few heavily reddened objects on the faint side. Restricting the sample to those with $B_{\rm max}-V_{\rm max}<0.20$ mag, the mean value of $M^V_{\rm max}$ as well as that of Δm_{15} is found to be comparable for the HV and Normal SNe Ia. Despite these similarities, the $B_{\rm max}-V_{\rm max}$ colors of the two groups show noticeable differences (see Fig. 3c), with the average value of the HV group being redder by $\sim$0.08 mag. This difference increases to 0.10 mag by further restricting the subsamples to those with $1.0\lesssim\Delta m_{15}\lesssim1.5$. In addition, the frequency of the Normal SNe Ia at the bluer end ($B_{max}-V_{max}<0$) is obviously higher than that of the HV objects, e.g., 43.6% vs. 14.5%. This indicates that the HV SNe Ia may preferentially occur in dusty environments, or they have intrinsically red colors (see discussion in §4). On the other hand, the morphological distributions of the host galaxies for these two groups do not show significant differences, perhaps suggesting that the color differences might not be caused by dust on large scales.

Although our analysis involves a large sample, we caution that the distributions of the above observables may suffer from an observational bias inherited in the observed sample. Further studies will be needed to determine whether this is indeed the case.

3.2. *Dust Absorption and Luminosity Standardization*

Dust absorption may be one of the main uncertainties in the brightness corrections of SNe Ia, depending not only on knowledge of the reddening $E(B-V)$ but also on the properties of the dust. Infrared photometry, together with optical data, would set better constraints on R_V (defined to be $A_V/E(B-V)$) on an object-by-object basis, but it was not available for most of our sample. Given the sample size, we attempt to quantify the average extinction ratio R_V for SNe Ia in a statistical way.

With the known empirical relations between the intrinsic colors and the decline rate Δm_{15} (Wang et al. 2009), we derive the reddening for our sample from the $B_{\rm max}-V_{\rm max}$ color and that measured at 12 days past the B maximum (X. Wang et al. 2005). To maintain consistency in our reddening determination, we did not use the tail color (Phillips et al. 1999) or the color at $t=35$ day after B maximum (Jha et al. 2007) owing to the possible abnormal color evolution of HV SNe Ia in the nebular phase (W08a). The host-galaxy reddening $E(B-V)_{\rm host}$ was taken to be the weighted average of the determinations by the above two methods, and the negative values were kept as measured. We note, however, that part of the reddening derived for the HV objects would be biased if their intrinsic color-Δm_{15} relations were different from those defined by the normal ones. Thus, the inferred value of R_V for them (discussed below) may not represent the true extinction ratio.

In Figure 4, the absolute peak magnitudes $M^V_{\rm max}$, corrected for the dependence on Δm_{15} using a relation derived from the low-reddening subsample, is plotted versus $E(B-V)_{\rm host}$. One can see that the HV group follows a relation significantly different from that for the Normal group. Assuming that the correlation is governed by dust absorption, the effective R_V values for these two groups are 1.57 ± 0.08 (HV) and 2.36 ± 0.09 (Normal). The objects with $z<0.010$ but without Cepheid distances were not included in the fit[9]. We note that SN 1996ai and SN 2003cg may have R_V close to 1.9, perhaps due to abnormal interstellar dust, although their distances have large

[9] SN 2006lf was excluded from the fit. After correction for the Galactic reddening $E(B-V)_{\rm Gal}=0.97$ mag with $R_V=3.1$, the V-band luminosity is found to be higher than that of the typical SN Ia by about 0.7 mag, possibly indicating a large uncertainty in the correction for Galactic reddening.

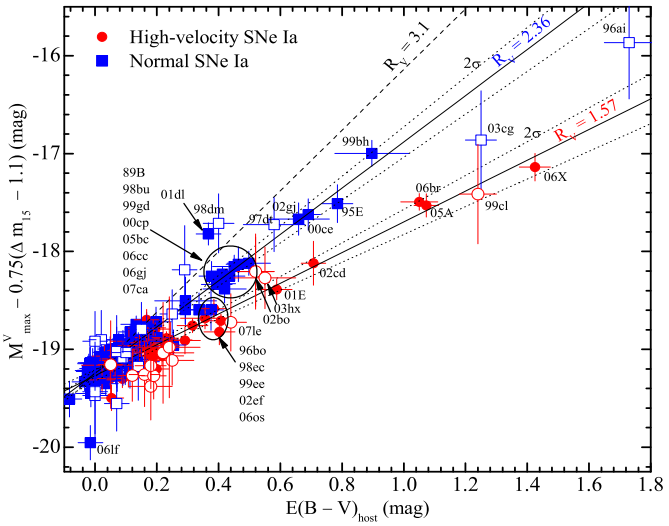

FIG. 4.— The Δm_{15}-corrected absolute V mag at maximum brightness versus the host-galaxy reddening. The filled symbols are SNe with $z \gtrsim 0.01$ or Cepheid-based distances, and the open symbols are nearby objects that were not included in the fit. The two solid lines show the best-fit R_V for SNe in the HV and Normal groups, with dotted lines indicating 2σ uncertainties. The dashed line represents the Milky Way reddening law.

uncertainties. It is not clear whether they are outliers, or a low R_V value is common for extremely reddened SNe Ia. Nevertheless, the slopes of the fits to the HV and Normal SNe Ia are still clearly different even if all the events with $E(B-V)_{\rm host} > 0.50$ mag are excluded. To examine the robustness of our analysis, we separate our sample using a 4σ selection criterion. This gives best-fit values of R_V as 1.53 ± 0.07 for the 25 hubble-flow HV SNe Ia and 2.32 ± 0.08 for the remaining 100 objects, consistent with the values determined from the 3σ subsamples.

The corresponding regression of $M^V_{\rm max}$ with two variables, Δm_{15} and $E(B-V)_{\rm host}$ takes the form

$$M^V_{max} = M_{\rm zp} + \alpha(\Delta m_{15} - 1.1) + R_V E(B-V)_{\rm host}, \quad (1)$$

where $M_{\rm zp}$ represents the mean absolute magnitude, corrected for the reddening in the Milky Way and the host galaxy, and normalized to $\Delta m_{15} = 1.1$. For the HV and Normal SNe Ia, one obtains

$$\begin{aligned} \text{Normal}: \alpha = 0.77 \pm 0.06, R_V = 2.36 \pm 0.07, \\ M_{\rm zp} = -19.26 \pm 0.02, N = 83, \sigma = 0.123; \end{aligned} \quad (2)$$

$$\begin{aligned} \text{HV}: \alpha = 0.75 \pm 0.11, R_V = 1.58 \pm 0.07, \\ M_{\rm zp} = -19.28 \pm 0.03, N = 42, \sigma = 0.128. \end{aligned} \quad (3)$$

The improved solutions are quite close to the provisional values. The resulting $M^V_{\rm max}$–Δm_{15} relation does not show a significant difference between the HV and Normal groups, and both slopes are found to be in accord with that adopted in the earlier analysis.

After accounting for the dependence on the two variables Δm_{15} and $E(B-V)_{\rm host}$, we find the luminosity scatter to be 0.128 mag for the HV group and 0.123 mag for the Normal one. A two-component fit to these two groups having different values of R_V yields a luminosity scatter 0.125 mag. Assuming a single best-fit $R_V = 1.85$, however, the luminosity scatter increases to 0.178 mag. We further performed the analysis using a subsample with $1.0 \lesssim \Delta m_{15} \lesssim 1.5$, which yields the best-fit R_V as 2.28±0.09 (Normal) and 1.54±0.08 (HV), respectively. This demonstrates that our results are not affected by objects at the extreme ends. Replacing the reddening term in Eq.(1) with the $B_{\rm max} - V_{\rm max}$ color, the best-fit slopes are found to be 2.29±0.08 (Normal) and 1.55±0.06 (HV). Such a dichotomy is also required for the pure color-term corrections, which can decrease the luminosity scatter from 0.177 mag to 0.136 mag. We thus propose that applying two different R_V values to the brightness corrections of SNe Ia is potentially beneficial, significantly decreasing the uncertainties in their distance measurements.

4. DISCUSSION AND CONCLUSIONS

We demonstrate that the standardization of SNe Ia can be noticeably improved by separating them into Normal and HV groups using a spectroscopic criterion (the blueshift of the absorption minimum of Si II λ6355). The main advantage of such a distinction is that SNe Ia of these two groups may have different extinction laws, though the R_V inferred for the HV SNe Ia might be partially biased due to the possibly different colors. By contrast with the Normal SNe Ia, the HV objects are found to have red $B-V$ color. This difference could be due to reddening, intrinsic color variance, observational bias, or a combination of these factors.

In the dust scenario, an additional absorption component, such as circumstellar (CS) dust (L. Wang et al. 2005), may be required to account for the paucity of HV SNe Ia at the bluest end (see Table 1 and Fig. 4). Tantalizing evidence for the presence of CS material around HV SNe Ia is provided by the detection of variable Na I D absorption lines in SN 2006X and 1999cl (Patat et al. 2007; Wang et al. 2008b; Blondin et al. 2009). The lower value of R_V might be naturally explained by multiple scattering in the CS dust shell (Goobar 2008).

As an alternative to reddening, the red $B-V$ color seen in the HV SNe Ia may be intrinsic, at least partially. Possible causes include the metallicity (Dominguez et al. 2001; Timmes et al. 2003) and a different extent of the burning front in the outer layers (Benetti et al. 2004). Increasing the metallicity of the progenitor could lead to a slightly redder $B-V$ color due to line blanketing; on the other hand, the increased opacity, as a result of the density enhancement in the outer ejecta, may also lead to a red color because of a low photospheric temperature at the earlier phases. A quantitative analysis would help determine whether the differences in the color as well as the inferred R_V values could be reproduced by the above two scenarios.

We emphasize that regardless of the origin of this color difference, the improvement in the distances to SNe Ia by applying two values of R_V will persist, e.g., with an uncertainty decreasing from ∼9% to 6%. Analysis of the impact of our findings on current cosmological studies will be presented in a forthcoming paper.

We thank Mark Phillips for allowing us to use the photometric parameters of SN 2005A before publication, D. C. Leonard for useful discussions, and the Lick Observatory staff for their assistance with the observations. C. V.

Griffith, J. J. Kong, N. Lee, and E. Miller helped maintain and improve the SN Database of A.V.F.'s supernova group at UC Berkeley. We are grateful to many students, postdocs, and other collaborators who have contributed to observations and reductions of our SN spectra and images over the past two decades, especially C. Anderson, A. J. Barth, L.-B. Desroches, G. Foster, B. Grigsby, N. Joubert, D. C. Leonard, T. Matheson, M. Moore, M. Papenkova, S. Park, B. Swift, T. Pritchard, and D. Winslow. This group is supported by NSF grant AST–0607485, the TABASGO Foundation, US Department of Energy SciDAC grant DE-FC02-06ER41453, and US Department of Energy grant DE-FG02-08ER41563. We are also grateful to the National Natural Science Foundation of China (10673007), and the China-973 Program 2009CB824800. The work of L. Wang is supported by NSF grant AST-0708873. KAIT and its ongoing operation were made possible by donations from Sun Microsystems, Inc., the HP Company, AutoScope Corporation, Lick Observatory, the NSF, the University of California, the Sylvia & Jim Katzman Foundation, and the TABASGO Foundation. We made use of the NASA/IPAC Extragalactic Database (NED), which is operated by the Jet Propulsion Laboratory, California Institute of Technology, under contract with NASA.

REFERENCES

Altavilla, G., et al. 2007, A&A, 475, 585
Barbon, R., et al. 1990,A&A, 237, 79
Benetti, S., et al. 2004, MNRAS, 348, 261
Benetti, S., et al. 2005, ApJ, 623, 1011 (B05)
Blondin, S., et al. 2009, ApJ, 693, 207
Branch, D., Dang, L., & Baron, E. 2009, PASP, 121, 238
Branch, D., et al. 1983, ApJ, 270, 123
Branch, D., et al. 2003, AJ, 126, 1489
Branch, D., et al. 2006, PASP, 118, 560
de Vaucouleurs, G., et al., 1991, Third Reference Catalogue of Bright Galaxies (New York: Springer-Verlag) (RC3)
Dominguez, I., Höflich, P., & Starniero, O. 2001, ApJ, 557, 279
Elias-Rosa, N., et al. 2006, MNRAS, 369, 1880
Filippenko, A. V., et al. 1992a, ApJ, 384, L15
Filippenko, A. V., et al. 1992b, AJ, 104, 1543
Filippenko, A. V. 1997, ARA&A, 35, 309
Filippenko, A. V., et al. 2001, in Small Telescope Astronomy on Global Scales, ed. B. Paczyński, W.-P. Chen, & C. Lemme (San Francisco: ASP), 121
Garavini, G., et al. 2007, A&A, 471, 527
Gerardy, C., et al. 2004, ApJ, 607, 391
Goobar, A. 2008, ApJ, 686, L103
Hachinger, S., et al. 2006, MNRAS, 2006, 370, 299
Hamuy, M., et al. 2002, AJ, 124, 417
Hicken, M., et al. 2009 (arXiv:0901.4787)
Hillebrandt, W., & Niemeyer, J. C. 2000, ARA&A, 38, 191
Jha, S., Riess, A. G., & Kirshner, R. P. 2007, ApJ, 659, 122
Komatsu., E., et al. 2009, ApJS, 180, 330
Kotak, R., et al. 2005, A&A, 436, 1021
Li, W., et al. 2003, PASP, 115, 453
Matheson, T., et al. 2008, AJ, 135, 1598 (M08)
Nugent, P., et al. 1995, ApJ, 455, L147
Pastorello, A., et al. 2007, MNRAS, 377, 1531
Patat, F., et al. 1996, MNRAS, 278, 111
Patat, F., et al. 2007, Science, 317, 924
Perlmutter, S., et al. 1999, ApJ, 517, 565
Phillips, M. M. 1993, ApJ, 413, L105
Phillips, M. M., et al. 1999, AJ, 118, 1766
Pignata, G., et al. 2008, MNRAS, 388, 971
Riess, A. G., et al. 1998, AJ, 116, 1009
Schlegel, D. J., Finkbeiner, D. P., & Davis, M. 1998, ApJ, 500, 525
Stanishev, V., et al. 2007, A&A, 469, 645
Suntzeff, N. B. 1996, in Supernovae and Supernova Remnants, ed. R. McCray & Z. Wang (Cambridge: Cambridge Univ. Press), 41
Tanaka, M., et al. 2008, ApJ, 677, 448
Timmes, F. X., Brown, E. F., & Truran, J. W. 2003, ApJ, 590, L83
Wang, L., et al. 2005, ApJ, 635, L33
Wang, L., et al. 2006, ApJ, 653, 490
Wang, X., et al. 2005, ApJ, 620, L87
Wang, X., et al. 2006, ApJ, 645, 488
Wang, X., et al. 2008a, ApJ, 675, 626 (W08a)
Wang, X., et al. 2008b, ApJ, 677, 1060
Wang, X., et al. 2009, ApJ, 697, 380
Yamanaka, M., et al. 2009, PASJ, in press (arXiv:0904.2763)

TABLE 1
Observed Parameters of the SN Ia Sample*.

SN	$v_{3K/220}$(km s^{-1})	$M^V_{\rm max}$(mag)	Δm_{15}‡(mag)	$B_{\rm max}-V_{\rm max}$(mag)	$E(B-V)_{\rm host}$(mag)	T(RC3)	SN type
1989B†	549	-18.15(0.15)	1.35(0.05)	0.32(0.07)	0.39(0.05)	3	N
1990N†	1179	-19.09(0.14)	1.05(0.05)	0.00(0.05)	0.11(0.04)	4	N
1994ae†	1575	-19.35(0.15)	0.89(0.05)	-0.05(0.05)	0.04(0.04)	5	N
1994D	1179	-19.26(0.57)	1.31(0.05)	-0.08(0.05)	-0.04(0.04)	-2	N
1995D	2129	-19.18(0.31)	1.02(0.05)	-0.02(0.05)	0.09(0.04)	-1	N
1995E	3496	-17.48(0.19)	1.17(0.07)	0.70(0.05)	0.78(0.05)	3	N
1996ai	1174	-15.94(0.57)	1.00(0.08)	1.69(0.05)	1.75(0.08)	4	N
1996X	2120	-19.36(0.31)	1.34(0.05)	-0.01(0.05)	0.06(0.04)	-4	N
1997dt	2356	-17.72(0.29)	1.11(0.10)	0.50(0.10)	0.59(0.09)	5	N
1997E	4055	-18.73(0.18)	1.42(0.05)	0.02(0.11)	0.11(0.09)	-2	N
1998aq†	1514	-19.25(0.14)	1.05(0.05)	-0.11(0.04)	-0.02(0.04)	2	N
1998bu†	810	-18.36(0.14)	1.06(0.04)	0.33(0.04)	0.42(0.04)	2	N
1998dm	1976	-17.86(0.33)	0.91(0.05)	0.30(0.04)	0.39(0.05)	5	N
1998eg	7056	-18.84(0.11)	1.17(0.10)	0.00(0.08)	0.12(0.06)	6	N
1999bh	5295	-16.64(0.13)	1.57(0.20)	0.87(0.09)	0.90(0.12)	3	N
1999cp	3112	-19.28(0.21)	1.02(0.03)	0.01(0.03)	0.07(0.04)	6	N
1999dg	6782	-18.97(0.10)	1.45(0.08)	-0.05(0.06)	0.02(0.04)	-2	N
1999ee	3163	-18.70(0.21)	0.96(0.05)	0.29(0.04)	0.38(0.04)	4	N
1999ej	4630	-18.70(0.14)	1.54(0.05)	0.00(0.04)	0.03(0.04)	0	N
1999gd	5775	-18.10(0.12)	1.13(0.10)	0.41(0.08)	0.50(0.07)	2	N
2000ca	7080	-19.39(0.10)	0.96(0.05)	-0.09(0.04)	0.02(0.04)	5	N
2000ce	4940	-17.74(0.17)	1.00(0.10)	0.59(0.16)	0.66(0.12)	3	N
2000cf	10930	-18.90(0.07)	1.43(0.05)	-0.02(0.04)	0.04(0.05)	···	N
2000cn	6958	-18.53(0.10)	1.57(0.05)	0.18(0.04)	0.20(0.05)	6	N
2000cp	10341	-18.16(0.12)	1.10(0.10)	0.37(0.14)	0.45(0.07)	2	N
2000cw	8692	-18.77(0.08)	1.26(0.05)	0.01(0.03)	0.14(0.08)	4	N
2000dk	4932	-18.93(0.14)	1.66(0.03)	-0.01(0.04)	-0.01(0.04)	-5	N
2000dm	4393	-18.88(0.15)	1.45(0.06)	-0.05(0.04)	-0.01(0.04)	2	N
2000dn	9248	-18.99(0.08)	1.04(0.06)	0.00(0.04)	0.11(0.04)	-1	N
2000dr	5332	-18.52(0.13)	1.73(0.05)	0.10(0.04)	0.05(0.04)	-1	N
2001ba	9194	-19.31(0.08)	0.98(0.05)	-0.10(0.04)	0.01(0.04)	3.7	N
2001bf	4556	-19.38(0.14)	0.79(0.04)	0.00(0.04)	0.10(0.04)	-3	N
2001bg	2273	-18.64(0.29)	1.10(0.04)	0.15(0.04)	0.26(0.04)	3	N
2001bt	4332	-18.84(0.15)	1.25(0.05)	0.15(0.07)	0.25(0.04)	4	N
2001cj	7507	-19.20(0.09)	0.93(0.04)	-0.08(0.04)	0.01(0.04)	6	N
2001ck	10583	-19.10(0.07)	0.99(0.04)	-0.04(0.04)	0.06(0.04)	3	N
2001cp	6714	-19.29(0.10)	0.85(0.05)	0.01(0.05)	0.13(0.04)	4	N
2001dl	5875	-18.01(0.11)	0.85(0.05)	0.26(0.04)	0.37(0.04)	8	N
2001el	1030	-18.12(0.65)	1.16(0.05)	0.06(0.04)	0.20(0.06)	6	N
2001ep	3881	-18.88(0.17)	1.43(0.05)	0.02(0.03)	0.14(0.06)	3	N
2001fe	4344	-19.30(0.15)	1.03(0.10)	0.03(0.04)	0.11(0.05)	1	N
2001fh	3630	-19.25(0.18)	1.45(0.04)	-0.16(0.05)	-0.08(0.04)	3	N
2002aw	7850	-19.04(0.09)	1.22(0.08)	0.05(0.04)	0.14(0.07)	3	N
2002cr	3112	-19.07(0.21)	1.21(0.05)	-0.01(0.03)	0.10(0.05)	6	N
2002dp	3133	-18.82(0.21)	1.25(0.05)	0.05(0.04)	0.16(0.04)	5	N
2002eb	7910	-19.19(0.09)	0.92(0.03)	-0.07(0.04)	0.07(0.04)	4	N
2002el	8337	-19.16(0.08)	1.25(0.08)	-0.03(0.06)	0.07(0.04)	-3	N
2002er	2804	-18.92(0.23)	1.32(0.03)	0.12(0.03)	0.23(0.04)	1	N
2002fk	2007	-18.95(0.33)	1.06(0.03)	-0.1 (0.04)	0.00(0.04)	4	N
2002ha	3913	-18.96(0.17)	1.34(0.07)	-0.08(0.03)	-0.02(0.04)	4	N
2002he	7447	-18.92(0.09)	1.32(0.06)	0.04(0.04)	0.10(0.04)	-5	N
2002hu	11460	-19.36(0.06)	1.05(0.07)	-0.11(0.05)	0.02(0.05)	5	N
2002hw	4896	-18.03(0.14)	1.57(0.10)	0.39(0.08)	0.42(0.07)	5	N
2002jg	4158	-17.31(0.16)	1.52(0.05)	0.64(0.04)	0.69(0.04)	5	N
2003cg	1340	-16.77(0.50)	1.22(0.10)	1.17(0.05)	1.23(0.05)	4	N
2003du	2307	-19.01(0.28)	0.97(0.06)	-0.09(0.04)	0.02(0.04)	8	N
2003gt	4407	-19.08(0.15)	1.01(0.03)	0.01(0.04)	0.10(0.04)	2	N
2003he	7287	-18.92(0.09)	1.01(0.05)	0.05(0.04)	0.15(0.04)	4	N
2003hv	1525	-19.15(0.43)	1.39(0.07)	-0.10(0.06)	0.00(0.04)	-2	N
2003kf	2085	-19.09(0.32)	1.01(0.08)	0.02(0.09)	0.06(0.05)	3	N
2004at	7082	-19.23(0.09)	1.10(0.03)	-0.10(0.04)	-0.02(0.04)	3	N
2004bd	2965	-17.99(0.24)	1.78(0.10)	0.37(0.14)	0.29(0.10)	1	N
2004bw	6553	-19.03(0.10)	1.27(0.06)	-0.03(0.04)	0.02(0.04)	5	N
2004eo	4421	-18.95(0.15)	1.43(0.03)	-0.01(0.03)	0.06(0.04)	2	N
2004ey	4438	-19.17(0.15)	1.17(0.07)	-0.09(0.06)	0.00(0.04)	5	N
2004fz	4935	-19.28(0.14)	1.32(0.07)	-0.07(0.06)	-0.01(0.05)	5	N
2004gs	8249	-18.32(0.08)	1.67(0.10)	0.11(0.04)	0.13(0.05)	-2?	N
2004S	2955	-18.99(0.22)	1.10(0.07)	-0.04(0.06)	0.07(0.04)	5	N
2005am	2308	-18.97(0.29)	1.52(0.08)	0.09(0.06)	0.12(0.04)	1	N
2005bc	3831	-17.82(0.18)	1.52(0.05)	0.43(0.07)	0.46(0.04)	3	N
2005bo	4504	-18.58(0.15)	1.12(0.07)	0.20(0.06)	0.29(0.05)	2	N
2005cf	2112	-19.13(0.31)	1.05(0.03)	-0.02(0.05)	0.11(0.03)	-2	N
2005de	4460	-18.70(0.15)	1.19(0.05)	0.04(0.04)	0.17(0.05)	···	N
2005el	4465	-19.09(0.15)	1.24(0.03)	-0.08(0.03)	-0.02(0.03)	-2	N

TABLE 1 — *Continued*

SN	$v_{3K/220}$(km s^{-1})	$M^V_{\rm max}$(mag)	$\Delta m_{15}{}^{\ddagger}$(mag)	$B_{\rm max} - V_{\rm max}$(mag)	$E(B-V)_{\rm host}$(mag)	T(RC3)	SN type
2005hc	13500	-19.04(0.06)	0.98(0.05)	-0.06(0.06)	0.08(0.04)	···	N
2005iq	9879	-18.91(0.07)	1.09(0.08)	-0.03(0.04)	0.08(0.04)	1	N
2005kc	4167	-18.49(0.17)	1.24(0.10)	0.25(0.07)	0.34(0.05)	2	N
2005ki	6111	-19.14(0.11)	1.22(0.05)	-0.03(0.05)	0.03(0.04)	-3	N
2005lz	13200	-18.90(0.07)	1.37(0.10)	0.07(0.05)	0.12(0.05)	···	N
2005ms	7771	-19.07(0.09)	0.83(0.07)	-0.02(0.05)	0.13(0.04)	···	N
2005na	8044	-19.24(0.09)	1.23(0.07)	-0.14(0.05)	-0.03(0.04)	1	N
2006ax	5387	-19.36(0.12)	1.08(0.04)	-0.05(0.03)	0.03(0.04)	3.5	N
2006az	9435	-19.11(0.08)	1.30(0.05)	-0.07(0.04)	0.00(0.04)	···	N
2006cc	9793	-18.26(0.07)	1.06(0.05)	0.35(0.03)	0.41(0.04)	···	N
2006D	2680	-18.82(0.25)	1.38(0.09)	0.03(0.06)	0.11(0.05)	2	N
2006dm	6240	-18.77(0.11)	1.56(0.05)	0.01(0.04)	0.04(0.03)	5	N
2006en	9234	-18.90(0.08)	0.99(0.06)	0.01(0.05)	0.11(0.04)	6	N
2006gj	8310	-18.03(0.09)	1.40(0.17)	0.36(0.09)	0.44(0.05)	2	N
2006hb	4601	-18.64(0.15)	1.67(0.08)	0.06(0.06)	0.08(0.04)	-3	N
2006kf	6240	-18.86(0.11)	1.52(0.07)	-0.03(0.06)	0.02(0.04)	···	N
2006lf	3889	-19.92(0.18)	1.15(0.05)	-0.04(0.06)	-0.02(0.04)	···	N
2006N	4278	-18.83(0.16)	1.55(0.07)	-0.01(0.07)	-0.02(0.04)	···	N
2006ob	17477	-18.84(0.05)	1.60(0.12)	0.05(0.04)	0.05(0.05)	3	N
2006S	9875	-18.98(0.07)	0.93(0.04)	0.05(0.03)	0.17(0.04)	···	N
2006td	4512	-18.41(0.15)	1.50(0.12)	0.12(0.05)	0.20(0.05)	···	N
2007af	1918	-19.08(0.34)	1.22(0.05)	0.04(0.03)	0.15(0.04)	6	N
2007bc	6555	-18.95(0.11)	1.30(0.08)	-0.04(0.06)	0.05(0.04)	1	N
2007bm	1996	-18.22(0.33)	1.20(0.09)	0.46(0.06)	0.55(0.04)	5	N
2007ca	4521	-18.39(0.15)	0.91(0.05)	0.29(0.04)	0.38(0.04)	5	N
2007ci	5762	-18.71(0.12)	1.77(0.09)	0.02(0.06)	-0.02(0.04)	-5	N
2007F	7244	-19.15(0.09)	0.95(0.07)	-0.05(0.04)	0.06(0.04)	6	N
2007O	10969	-19.17(0.08)	1.12(0.08)	-0.04(0.07)	0.05(0.04)	5	N
2008bf	6647	-19.18(0.11)	1.03(0.06)	0.04(0.06)	0.12(0.04)	-5	N
1981B†	1179	-18.96(0.15)	1.11(0.10)	0.04(0.06)	0.17(0.07)	4	HV
1983G	1497	-18.90(0.45)	1.30(0.10)	0.17(0.10)	0.23(0.09)	-2	HV
1984A	1179	-18.91(0.57)	1.20(0.10)	0.16(0.08)	0.26(0.08)	1	HV
1989A	2756	-19.17(0.25)	1.05(0.10)	0.10(0.10)	0.23(0.09)	4	HV
1992A	1338	-18.90(0.50)	1.47(0.05)	-0.01(0.04)	0.04(0.04)	-2	HV
1996bo	4893	-18.69(0.14)	1.28(0.06)	0.30(0.05)	0.40(0.05)	5	HV
1997bp	2647	-19.09(0.25)	1.13(0.05)	0.16(0.05)	0.28(0.07)	1	HV
1997do	3140	-19.00(0.22)	1.10(0.07)	0.05(0.07)	0.14(0.07)	4	HV
1998dh	2766	-19.18(0.24)	1.22(0.04)	0.08(0.03)	0.20(0.04)	5	HV
1998dk	3609	-18.94(0.19)	1.05(0.10)	0.15(0.07)	0.24(0.07)	5	HV
1998ec	6032	-18.61(0.13)	1.19(0.10)	0.28(0.08)	0.36(0.08)	3	HV
1998ef	5020	-19.40(0.13)	1.23(0.05)	-0.04(0.03)	0.05(0.04)	3	HV
1999cc	9452	-18.88(0.09)	1.48(0.10)	0.00(0.05)	0.06(0.06)	5	HV
1999cl	1179	-17.33(0.57)	1.22(0.05)	1.14(0.04)	1.23(0.06)	3	HV
1999dk	4181	-19.13(0.16)	1.15(0.05)	0.08(0.05)	0.17(0.04)	5	HV
2000fa	6533	-19.04(0.10)	0.89(0.05)	0.07(0.03)	0.17(0.04)	10	HV
2001ay	9269	-19.04(0.08)	0.72(0.05)	0.06(0.06)	0.32(0.05)	4	HV
2001br	6057	-18.52(0.11)	1.34(0.05)	0.09(0.03)	0.17(0.04)	1	HV
2001da	4790	-18.84(0.14)	1.20(0.05)	0.17(0.04)	0.29(0.05)	2	HV
2001E	6140	-18.41(0.11)	1.07(0.05)	0.50(0.05)	0.59(0.05)	5	HV
2001en	4478	-18.98(0.15)	1.28(0.05)	0.00(0.03)	0.06(0.05)	···	HV
2002bf	7418	-19.03(0.11)	1.00(0.10)	0.03(0.07)	0.17(0.06)	3	HV
2002bo	1547	-18.16(0.43)	1.16(0.03)	0.40(0.03)	0.51(0.06)	1	HV
2002cd	2919	-18.18(0.22)	1.02(0.06)	0.63(0.04)	0.71(0.04)	4	HV
2002cs	4592	-18.96(0.14)	1.05(0.03)	-0.04(0.03)	0.11(0.06)	-5	HV
2002cu	6889	-18.88(0.10)	1.42(0.05)	0.04(0.03)	0.12(0.04)	-5	HV
2002de	8474	-18.82(0.08)	1.05(0.03)	0.09(0.03)	0.19(0.04)	1	HV
2002dj	2825	-19.18(0.23)	1.08(0.03)	0.09(0.04)	0.18(0.05)	-5	HV
2002ef	6846	-18.60(0.10)	1.08(0.05)	0.33(0.05)	0.38(0.04)	-2	HV
2003cq	10117	-18.79(0.08)	1.37(0.05)	0.07(0.07)	0.19(0.04)	4	HV
2003hx	1994	-18.18(0.34)	1.23(0.10)	0.50(0.09)	0.55(0.08)	-1	HV
2003W	6334	-19.08(0.11)	1.08(0.05)	0.11(0.04)	0.22(0.07)	5	HV
2004as	9612	-18.85(0.07)	1.15(0.05)	0.10(0.04)	0.23(0.04)	···	HV
2004bk	7225	-19.24(0.10)	1.18(0.08)	0.03(0.06)	0.09(0.05)	3	HV
2004dt	5644	-19.25(0.12)	1.12(0.05)	0.00(0.04)	0.11(0.05)	1	HV
2004ef	8931	-18.76(0.08)	1.42(0.05)	0.05(0.04)	0.09(0.04)	3	HV
2005A	5502	-17.39(0.12)	1.28(0.03)	1.01(0.01)	1.07(0.04)	4.5	HV
2006ac	7180	-18.97(0.10)	1.23(0.08)	0.12(0.07)	0.19(0.05)	3	HV
2006bq	6432	-18.71(0.11)	1.57(0.06)	0.16(0.04)	0.17(0.04)	-2	HV
2006br	7657	-17.15(0.10)	1.55(0.15)	1.03(0.07)	1.05(0.06)	3	HV
2006bt	9737	-18.93(0.07)	1.12(0.05)	0.14(0.05)	0.23(0.04)	0	HV
2006cp	6991	-19.18(0.10)	1.13(0.05)	0.10(0.04)	0.20(0.04)	5	HV
2006ef	5102	-18.90(0.13)	1.37(0.05)	0.01(0.04)	0.06(0.04)	-1	HV
2006ej	5801	-18.85(0.12)	1.40(0.12)	-0.01(0.06)	0.03(0.04)	5	HV
2006gr	10037	-18.92(0.08)	0.93(0.05)	0.09(0.06)	0.19(0.05)	3	HV
2006le	5178	-19.48(0.13)	0.88(0.05)	-0.10(0.04)	0.02(0.04)	3	HV

TABLE 1 — *Continued*

SN	$v_{3K/220}$(km s^{-1})	$M^V_{\rm max}$(mag)	Δm_{15}‡(mag)	$B_{\rm max}-V_{\rm max}$(mag)	$E(B-V)_{\rm host}$(mag)	T(RC3)	SN type
2006os	9624	-18.45(0.07)	1.44(0.07)	0.30(0.04)	0.41(0.05)	···	HV
2006sr	6960	-18.88(0.11)	1.28(0.09)	0.07(0.06)	0.09(0.05)	6	HV
2006X†	957	-16.98(0.14)	1.31(0.05)	1.35(0.04)	1.42(0.05)	4	HV
2007bd	9581	-19.11(0.07)	1.35(0.12)	0.00(0.05)	0.05(0.04)	1	HV
2007co	7963	-18.91(0.09)	1.13(0.05)	0.08(0.04)	0.16(0.05)	···	HV
2007gi	1824	-19.06(0.36)	1.37(0.05)	0.15(0.05)	0.16(0.05)	-3	HV
2007le	2041	-18.78(0.32)	1.02(0.05)	0.37(0.04)	0.45(0.04)	5	HV
2007qe	7200	-19.09(0.10)	1.02(0.05)	0.10(0.05)	0.22(0.04)	···	HV
2007sr	1757	-19.31(0.38)	1.16(0.07)	0.11(0.08)	0.23(0.07)	9	HV

* Uncertainties are 1σ. See text for a discussion of recession velocities. Host-galaxy "T" types are from RC3.

† SN Ia with Cepheid distance.

‡ The Δm_{15} value has been corrected for the reddening effect (Phillips et al. 1999).